Performance study on the second-level muon trigger of the ATLAS experiment at the LHC

G. Artoni

"Sapienza" Università di Roma - Rome, Italy
INFN, Sezione di Roma 1 - Rome, Italy

Summary. — This article will discuss the status and the performances of the second-level muon trigger of the ATLAS experiment at the LHC; to perform these studies, data from the first collisions at $\sqrt{s} = 7$ TeV have been used.

PACS `29.20.-c` – Accelerators.
PACS `29.85.Ca` – Data acquisition and sorting.
PACS `29.90.+r` – Other topics in elementary-particle and nuclear physics experimental methods and instrumentation.

1. – Brief introduction to the ATLAS experiment

ATLAS is one of the four major experiments working at the LHC and, in particular, it is the biggest among them: 44 m in length and 25 m in height. It is a *general purpose* experiment and this means that it has to look for not just the Higgs boson missing from the Standard Model, but also for new particles in a range of energy that has never been explored so far. In order to accomplish this task, the detector has been designed in a way that many signatures are possibly reconstructed, thus allowing for various possible discoveries. The sub-detectors involved in the muon reconstruction chain are the following:

– *Inner Detector* - Around the beam pipe and with a radius of about 1 m we have the tracking system, divided into three different sub-detectors which use various technologies. They are the *Pixel Detector*, the *SemiConductor Tracker* and the *Transition Radiation Tracker*. These detectors are able, thanks to the presence of a 2 T solenoidal magnetic field, to reconstruct all charged-particles tracks with $|\eta| < 2.4$[1].

---

[1] In ATLAS it is defined a Cartesian coordinate system, having the z-axis along the beam

– *Calorimeters* - Immediately outside the *InnerDetector* there are the calorimeters of the experiment, the *Electromagnetic Calorimeter* and the *Hadronic Calorimeter* respectively. They have been designed to detect many physical signatures, such as photons, electrons and jets. Muons will also be seen by the calorimeters, but being minimum ionizing particles they will lose only about $2\,\mathrm{GeV}$(^{2}) of their energy and they will not be stopped in the detector.

– *Muon Spectrometer* - This is the farthest sub-detector in ATLAS, as muons have the peculiarity of being the only particle that passes through the whole detector. The *Muon Spectrometer* has been designed to reconstruct all these tracks using a toroidal magnetic field and different technologies have been used for different regions of the detector. In the region where $|\eta| < 1.05$, which is called the *barrel* region, we have *Resistive Plate Chambers* (*RPC*) to provide a fast identification of the muon and *Monitored Drift Tubes* (*MDT*) for the full reconstruction; the same happens in the *endcap* region where we have *Thin Gap Chambers* (*TGC*) for the trigger signals and *MDT*s plus *Cathode Strip Chambers* (*CSC*) for the reconstruction.

The second-level muon trigger will use all these sub-detectors to perform a selection; further details on the experiment can be found here [1].

2. – The ATLAS muon trigger

The ATLAS muon system is the biggest sub-detector of the whole experiment and it is capable of reconstructing muons in standalone mode or using the combination with the *Inner Detector* measurement. As all the trigger systems in ATLAS it is divided into three different levels, that go under the simple names of *Level 1* (L1), *Level 2* (L2) and *Event Filter* (EF). Here we will briefly explain how these three different levels work:

*L*1 - The first level has been designed to reduce the trigger rate from about $1\,\mathrm{GHz}$ to $200\,\mathrm{kHz}$. To accomplish this it uses only *RPCs* in the *barrel* and only TGCs in the *endcap*, since the total processing time available for this level is about $2.5\,\mu s$; this means that at the L1 the trigger is completely *hardware*. The task of the first level is to identify all those events in which there is at least one muon and then to pass the information about the region in which this muon was found (*Region of Interest*, RoI) to the L2.

*L*2 - The second level receives the RoI from the first level and uses *software*-based algorithms to reduce the trigger rate from $200\,\mathrm{kHz}$ to about $1\,\mathrm{kHz}$. In order to accomplish this it performs a simplified reconstruction of the muon track, using also precision data from the *MDTs*, just in the RoI flagged by the L1; this is necessary if we do not want this level to exceed the total processing time available. The final reconstructed muon is then passed to the last trigger level, the EF.

---

direction, the x-axis pointing towards the center of the accelerating ring and the y-axis pointing in the upper direction. These coordinates do not provide a good system for physics analysis at a hadronic collider and thus we tend to use the z coordinate, the ϕ coordinate which is the angle in the x-y plane and the θ coordinate, which is the angle in the y-z plane. Moreover, θ does not represent a good choice because it is not a Lorentz invariant with respect to boosts along the z-direction; this leads to the usage of another coordinate, $\eta = -\ln(\tan(\theta/2))$.
(^{2}) In this article we will use the convention $c = 1$, so all momenta will be given in units of GeV.

EF - The EF has to reduce the rate to about $100\,\mathrm{Hz}$, which is what we can then write on disk and save for further analysis; since there are about $2\,\mathrm{s}$ for processing, it is finally possible to reconstruct the event in the whole detector, starting from the RoI identified and refined by the L1 and the L2.

3. – The ATLAS second-level muon trigger

The second-level muon trigger is a chain of different algorithms, each one with a particular aim in the reconstruction. The first algorithm in the chain is μFast, then there is μComb and finally μIso; the total processing time available for these algorithms is about $10\,\mathrm{ms}$ and this forces us to simplify as much as possible all the operations performed by these algorithms.

3'1. *μFast*. – μFast, as the name suggests, is the algorithm dedicated to a fast reconstruction of the muon track within the muon spectrometer. It uses all the information coming from the L1 and selects hits from the *MDTs* performing a pattern recognition; after this it uses the *MDTs* drift times to perform a fit of the track and then a measurement of the p_T([3]) is given by a *Look-up-table*. Before passing the RoI to the next algorithm in the chain, μFast applies a cut on the p_T of the muon, thus rejecting muons of transverse momentum lower than the configured threshold.

3'2. *μComb*. – μComb has been developed to perform the combined reconstruction of the muon, using the track in the *Muon Spectrometer* and the tracks from the *Inner Detector*; it starts from μFast track and then extrapolates this back to the primary vertex, using a *Look-up-table*. After this it looks for the track in the *Inner Detector* that best matches in ΔR the back-extrapolated track. If a suitable track is found, μComb combines the parameters of the two tracks to give the new p_T, η and ϕ of the combined track. At last, a cut on this combined p_T is applied.

3'3. *μIso*. – The last algorithm of the chain is μIso, that has been designed to reject muons coming from jets or from semi-leptonic decays of kaons and pions. In order to accomplish this, two different ways of functioning for the algorithm have been prepared, one relying on the *Inner Detector*, and the other one on the *Electromagnetic* and *Hadronic Calorimeters*.

Track-based Algorithm - This configuration of the algorithm uses the *Inner Detector* tracks within the RoI to establish if the track is isolated or not. In particular it calculates this quantity:

$$(1) \qquad Iso = \Sigma^{\Delta R < 0.2} p_T - p_T^{\mu}(^4),$$

where p_T is measured in GeV. Of course isolated muons should have $Iso \simeq 0$ and a cut can be applied on this variable to preserve only muons with Iso under a particular threshold.

([3]) $p_T = \sqrt{p_x^2 + p_y^2}$ is the projection of the muon momentum on the x-y plane. It is very useful because we can apply conservation laws only in the x-y plane, given the fact that we cannot know the parton momentum along the z-direction.
([4]) $\Delta R = \sqrt{\Delta\eta^2 + \Delta\phi^2}$ is used to measure the distance between two tracks in the detector.

Calorimeter-based Algorithm - Another way of determining if the muon is isolated is to look at the calorimeter deposits around the muon track. The algorithm defines two different cones, one called Inner Cone and containing only those cells in which the muon has passed, and another one called Outer Cone, around the first one. For the Outer Cone is then evaluated this quantity:

$$(2) \qquad Iso = \Sigma_{cells}^{OuterCone} E_T - \Sigma_{cells}^{InnerCone} E_T(^5)$$

Looking at this variable it should be straightforward that isolated muons have $Iso \simeq 0$; we can then apply a cut to reject all muons having Iso greater than the configured threshold.

4. – Second-level muon trigger performances

In this section we will go through the performances of the various algorithms, measured on the first $94\,\mathrm{nb}^{-1}$ data collected by the ATLAS experiment in 2010.

4˙1. *Muon p_T resolution.* – As already pointed out in sect. **3**, μFast and μComb have been designed to reconstruct the track parameters of the muon, in the *Muon Spectrometer* only and combined with the *Inner Detector*, respectively, and then a hypothesis cut is applied on the muon transverse momentum. Thus a good resolution on this quantity is necessary for the trigger to work properly. To evaluate the p_T resolution we decided to use this quantity:

$$(3) \qquad r_{p_T} = \frac{1/p_T^{offline} - 1/p_T^{algo}}{1/p_T^{offline}} = 1 - \frac{p_T^{offline}}{p_T^{algo}} \, ,$$

where p_T^{algo} can be alternatively $p_T^{\mu Fast}$ or $p_T^{\mu Comb}$ and $p_T^{offline}$ is the p_T of the *offline* track, which is the best reconstruction available in the ATLAS experiment. It is easy to notice that, if everything is working as it should, r_{p_T} will be centered at zero, meaning that the energy scales of the *offline* algorithm and of the L2 algorithm are the same, and the width of the distribution should give us the resolution of the algorithm. It is possible to see this for $\mu Fast$ in fig. 1 and for $\mu Comb$ in fig. 2, for different ranges in η and in p_T. For what concerns $\mu Fast$, we notice that there is some unbalance between *offline* and $\mu Fast$ p_T, but this is well modeled by the Monte Carlo(^{6}), showing that the performance of the $\mu Fast$ algorithm are exactly as expected. In the *barrel* region, for $p_T > 6\,\mathrm{GeV}$, we can see that the width of the distribution from data is wider than that from Monte Carlo, indicating that the resolution of the algorithm is worse than expected. This small effect is due to the fact that the L2 muon trigger has never been tested on collision data at $\sqrt{s} = 7\,\mathrm{TeV}$ before and thus some discrepancies in terms of resolution are expected. Moving on to $\mu Comb$, we can see that there is a very good agreement between data and Monte Carlo, indicating that the algorithm is working exactly as expected. In the last

---

(^{5}) As for p_T, $E_T = \sqrt{E_x^2 + E_y^2}$.
(^{6}) The Monte Carlo sample used in this article is composed by minimum bias events, *i.e.* events for which minimal requirements have been imposed; for example one of these requirements was that a collision took place in the ATLAS detector and another one was that there was at least one track with $p_T > 500\,\mathrm{MeV}$.
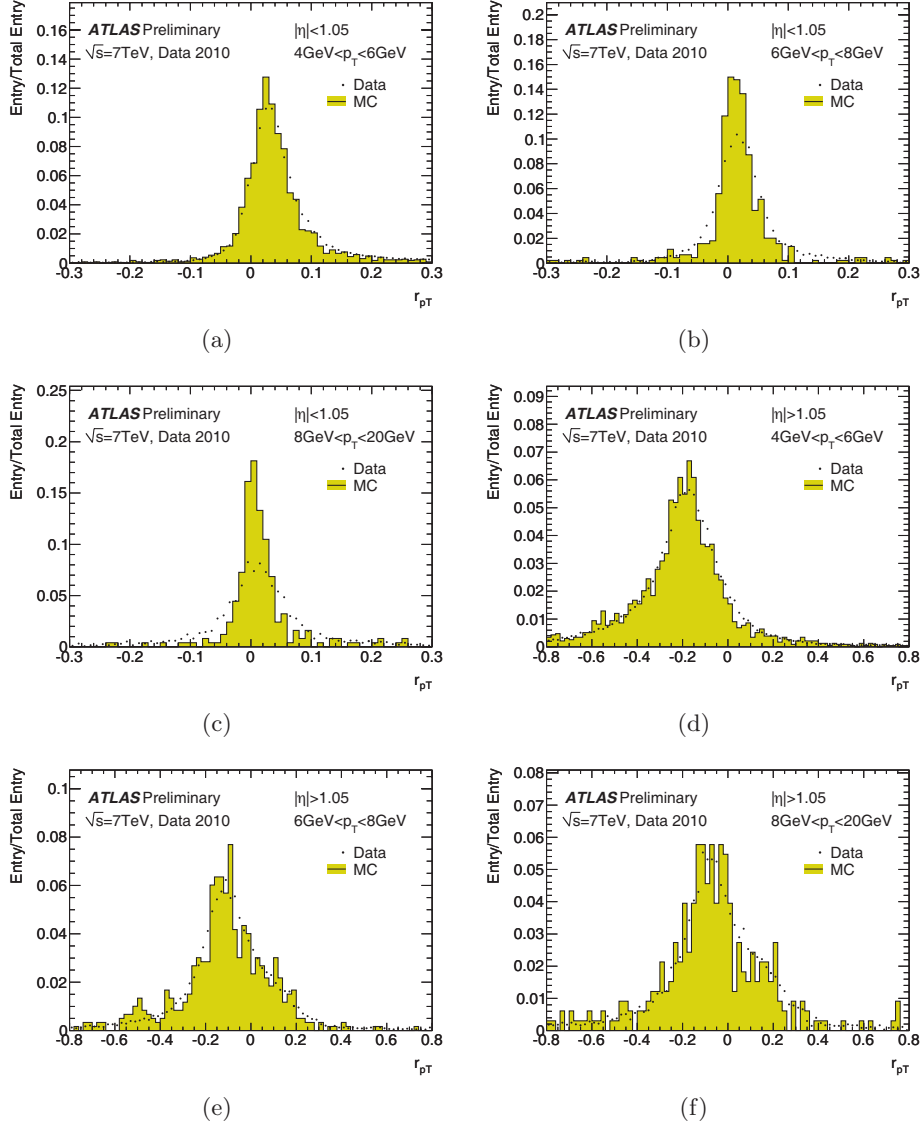
Fig. 1. – μFast p_T resolution, indicated by the variable r_{p_T} (see eq. (3)), for different regions and ranges in p_T: for the *barrel* region in (a), (b) and (c) while for the *endcap* region in (d), (e) and (f). Also (a) and (d) have been made for $4\,\text{GeV} < p_T < 6\,\text{GeV}$, (b) and (e) for $6\,\text{GeV} < p_T < 8\,\text{GeV}$ and (c) and (f) for $8\,\text{GeV} < p_T < 20\,\text{GeV}$.

plot on fig. 2 it is possible to see that the resolution from data is slightly worse than that from Monte Carlo and that the width of r_{p_T} grows with the muon transverse momentum, as it should be.

4˙2. *Efficiency.* – The purpose for which μFast and μComb have been designed is to reject muons below preconfigured thresholds in p_T and preserve all muons above these
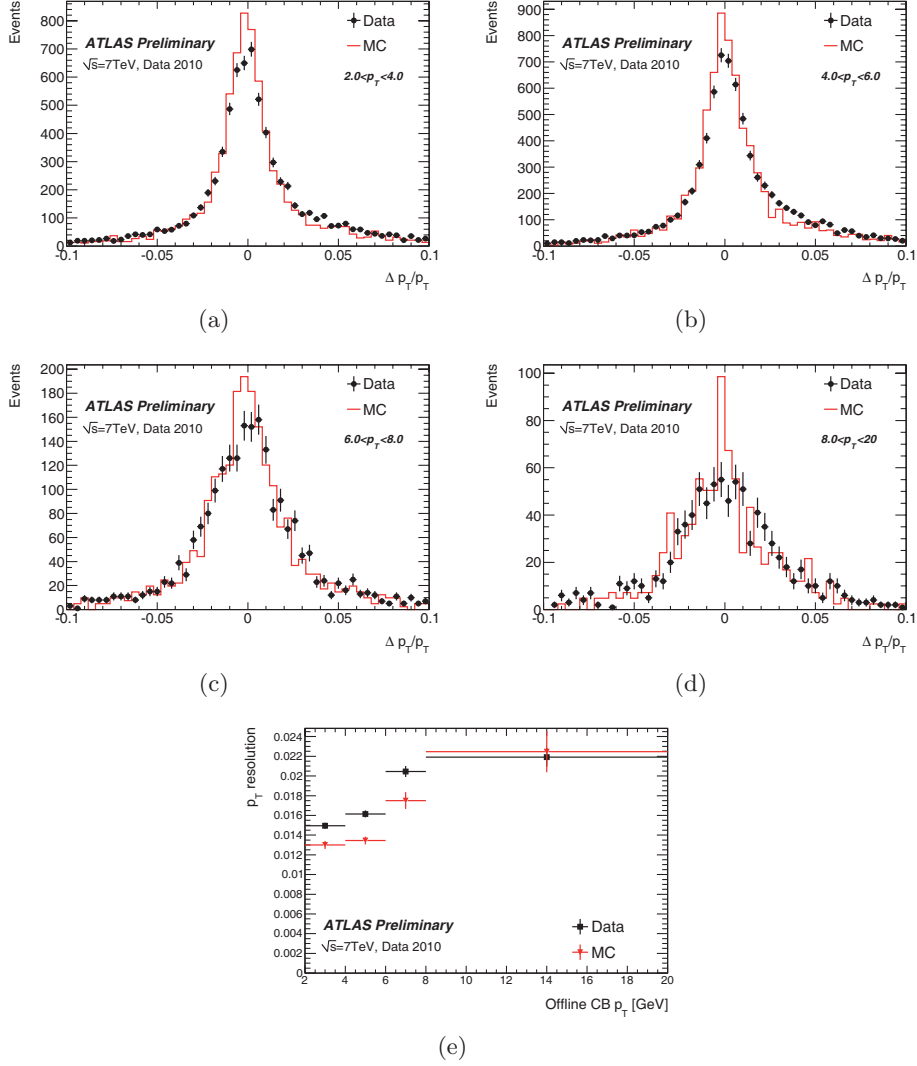
Fig. 2. – μComb p_T resolution, indicated by the variable r_{p_T} (see eq. (3)), for different ranges in p_T: (a) has been made for $2\,\text{GeV} < p_T < 4\,\text{GeV}$, (b) for $4\,\text{GeV} < p_T < 6\,\text{GeV}$, (c) for $6\,\text{GeV} < p_T < 8\,\text{GeV}$ and (d) for $8\,\text{GeV} < p_T < 20\,\text{GeV}$. The last plot, (e), shows the widths of the four previous distributions as a function of the *offline* p_T.

thresholds, in order to reduce the trigger rate without losing interesting high-p_T events. The efficiency of the p_T cut is then crucial in order to understand if the algorithm is working in the proper way and can then be used to reject events online, allowing the experiment to bear greater luminosities. The efficiency is evaluated as follows:

$$(4) \qquad \epsilon = \frac{\text{Number of events passing the } p_T \text{ cut}}{\text{Total events coming from the previous level}}$$
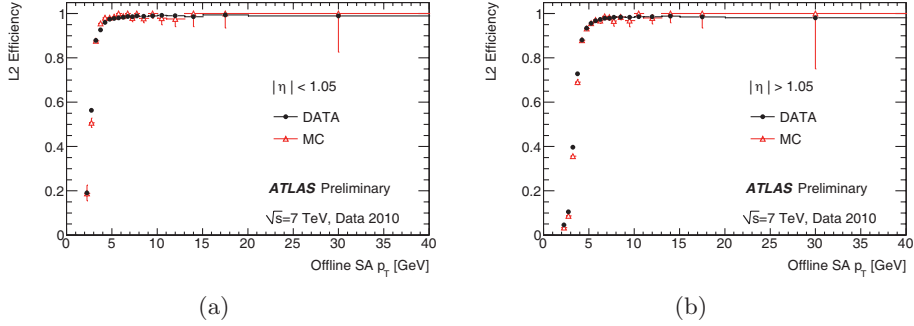
(a)   (b)

Fig. 3. – μFast efficiency curves as a function of p_T, for *barrel* in (a) and *endcap* in (b) with the threshold set at 4 GeV, with respect to the previous level, L1.

and it is easy to notice that we should have $\epsilon \simeq 0$ below the threshold and $\epsilon \simeq 1$ above threshold. We can see in fig. 3 the efficiency for μFast and in fig. 4 for μComb; we show here the *turn-on* curve as a function of the *offline* p_T in which there is a very good agreement between data and Monte Carlo, showing that the L2 is perfectly capable of rejecting events and is then reliable. We should note that the strange behavior in fig. 4(b) is due to the lack of events in that p_T region, thus producing effects that disappear with the increase of statistics.

4$^{.}$**3.** *μIso commissioning.* – So far we have showed only the performance of the first two algorithm in the chain of the second-level muon trigger. Here we show the first results on μIso, whose commissioning will be done in a second phase since its rejection is needed only at high luminosities (starting from $10^{32}\,\mathrm{cm}^{-2}\,\mathrm{s}^{-1}$). In fig. 5(a) we can see a very good agreement between data and Monte Carlo for the track-based isolation. It is possible to observe that the peak at zero represents those muons that are isolated and thus do not contain any other track in a cone of $\Delta R = 0.2$ around them. This criterium to establish if the muon is isolated or not will then be used in the experiment as soon as the trigger rate requires it, since it appears to be perfectly working. For what concerns
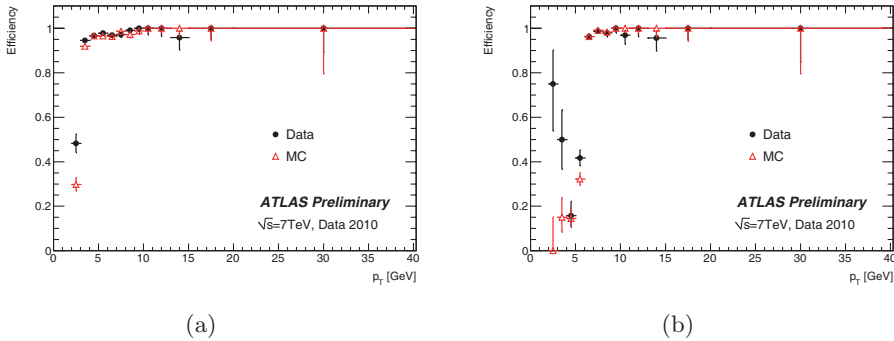

(a)   (b)

Fig. 4. – μComb efficiency curves as a function of p_T for two different thresholds, 4 GeV in (a) and 6 GeV in (b) with respect to the previous algorithm, μFast.
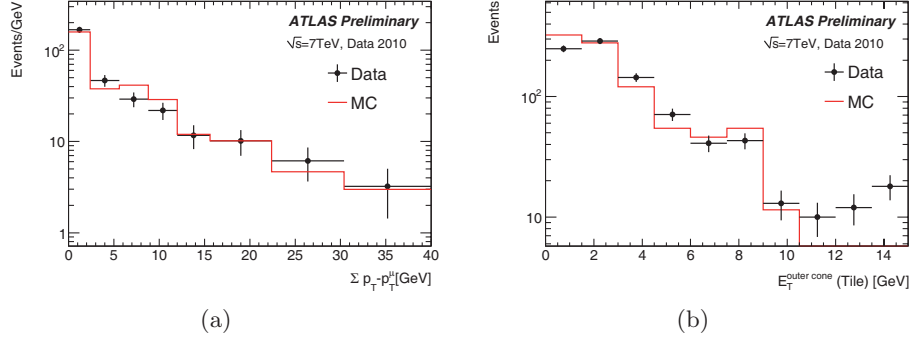
(a)   (b)

Fig. 5. – μIso reconstructed variables, $Iso = \Sigma^{\Delta R < 0.2} p_T - p_T^\mu$ in (a) for the track-based algorithm and $\Sigma_{cells}^{OuterCone} E_T$ in (b) for the calorimetric-based algorithm.

the calorimetric-based isolation, we can see in fig. 5(b) a plot showing the energy of all the cells in the Outer Cone of the *Hadronic Calorimeter*. In this case it appears to be a good agreement with Monte Carlo at low energies and some discrepancies at high energies, probably due to the lack of statistics.

4˙4. *Trigger rates*. – The last part of this article deals with the trigger rate issue, already explained in sect. **2**. In fig. 6(a) we can see different chains of triggers using different thresholds and their rate as a function of the instantaneous luminosity measured by ATLAS. We can notice that the rate exponentially grows with the instantaneous luminosity and this has allowed experts to predict the trigger rate for higher luminosities. For what concerns fig. 6(b), we show the rate reduction from the L1 (which is the ref-
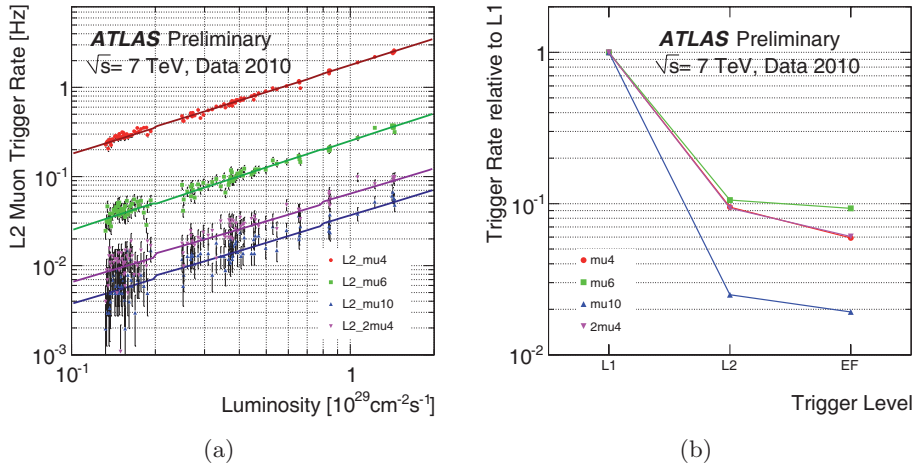

(a)   (b)

Fig. 6. – Trigger rate behavior for the first $94\,\mathrm{nb}^{-1}$ of data collected by ATLAS. In (a) it is possible to see the different trigger rates for various trigger chains: the number at the end of each chain indicates the p_T cut that the chain performs. In (b), instead, we can see the rate reduction induced by the L2 in the muon trigger.

erence) to the EF. We need to point out that the major part of the reduction has been done by the L2 trigger, as it is expected, and this shows once again the importance of this sub-system within the whole muon trigger system.

5. – Conclusions

In this article we have shown the first results obtained using collision data at $\sqrt{s} = 7$ TeV for the second-level muon trigger of the ATLAS experiment. We have explained how the whole trigger chain works and shown the measured performances of all the algorithms, in terms of resolutions (subsect. **4**˙1), efficiencies (subsect. **4**˙2) and reconstructed variables (subsect. **4**˙3). We have pointed out the good agreement between data and Monte Carlo and thus the very good behavior of all the algorithms, indicating that they are ready to be used online for rejecting events.

REFERENCES

[1] ATLAS COLLABORATION, *The ATLAS Experiment at the CERN Large Hadron Collider*, *JINST*, **3** S08003 (2008).